## Photoactivation dynamics in photosynthetic and signal transduction proteins studied by ultra-fast time-resolved spectroscopy

Bonetti, C.

2009

***document version***
Publisher's PDF, also known as Version of record

# Chapter 1 Light-harvesting and signal transduction proteins and their characteristic pigments; techniques, tools and methods for spectroscopic measurements and data analysis.

*Abbreviations*: ATP, Adenosine-Tri-Phosphate; NADPH, Nicotinamide-Adenine-Dinucleotide-Phosphate; LH, Light Harvesting; (B)Chl, (Bacterio)Chlorophylls; Chl-*a*, Chlorophyll-*a*; RC, Reaction Centre; Per, Peridinin; ISC, Inter System Crossing; ET, Energy Transfer; TEET, Triplet Excitation Energy Transfer; hECN, 3' -hydroxy-echinenone; PCP, Peridinin-Chlorophyll-*a* Protein; PSII, photosystem II; EET, Excitation Energy Transfer; NPQ, Non Photochemical Quenching; FAD, Flavin Adenine Dinucleotide; Y: osine; W, Tryptophan; Q, Glutamine; N, Asparagine; S, Serine; M, Methionine; I, Isoleucine; A, Alanine; Ti:S, titanium:sapphire; OD, Optical Density; NOPA, Non-collinear Optical Parametric Amplifier; FTIR, Fourier Transformed Infra-Red.

## Photosynthesis

Photosynthesis, from the Greek φώτο- (photo-) "light," and σύνθεσις (synthesis) "placing with", is the process that plants, some bacteria and algae use to convert Sun light energy into chemical energy (adenosine-tri-phosphate-ATP, or nicotinamide-adenine-dinucleotide-phosphate-NADPH) for both growth and energy storage [1, 2]. In this thesis we study exclusively the primary processes starting with photon absorption by one of the pigments in the light-harvesting (LH) antenna. There are two different classes of absorbing pigments involved in photosynthesis: (bacterio)chlorophylls and carotenoids. Upon absorption of a photon these molecules get promoted to an electronic excited state, which are characterized by lifetimes of nanoseconds or shorter (ns, $10^{-9}$ s) [3].

This energy must therefore be rapidly transferred to a special protein (Reaction Centre – RC) that is able to transform the short-lived excited state in a more stable, long-lived charge-separated state. Energy transfer among antenna pigments takes place in hundreds of femtoseconds (fs, $10^{-15}$ s) to picoseconds (ps, $10^{-12}$ s), energy transfer among antennas or from antenna to the RC takes place on the tens of picosecond time scale [4].

## Light-Harvesting pigments

Pigments are chemical compounds with the ability, once illuminated, to absorb light of certain visible wavelength and not-absorbing the remaining part of the (visible) radiation. Because they interact with light and are selective absorbers, pigments are useful to plants and other organisms that perform photosynthesis.

### Chlorophyll-*a* (Chl-*a*)

Chlorophyll [5, 6] is the primary light-harvesting absorber in photosynthesis and in addition acts as the primary electron donor in RC. With its tetrapyrrole geometry, Chl-*a* absorbs in the blue and red part of the visible spectrum (Figure 1). The peak near 430 nm is the so-called Soret band, the red-most absorption band, called $Q_y$-band, is located near 670 nm. Less evident in the spectrum is the weak $Q_x$ transition that appears near 630 nm [3, 5, 6]. Chlorophylls do not absorb yellow-green light, which gives these pigments their green color.

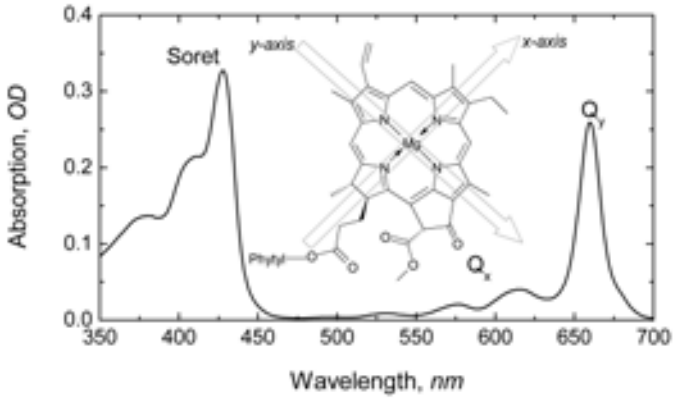


**Figure 1**: Structural formula of Chlorophyll-a and absorption spectrum in *n*-hexane.

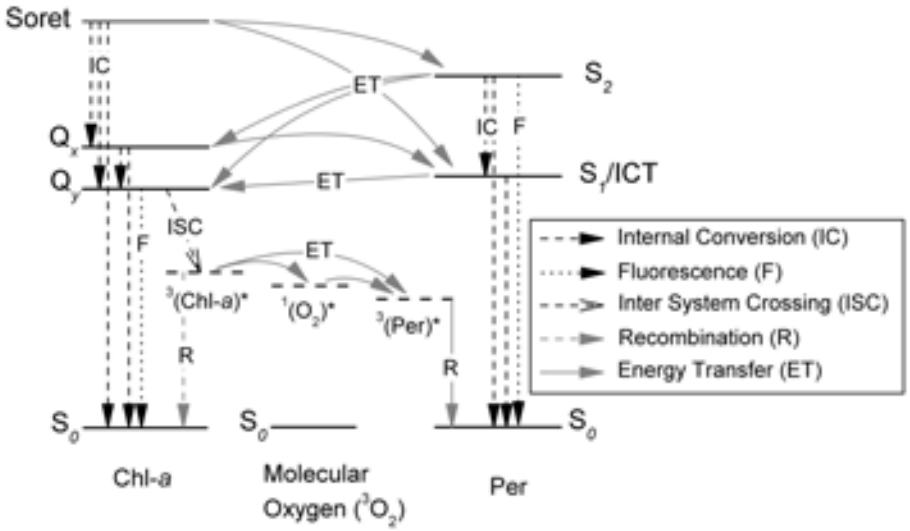


**Figure 2**: Energy diagram for the photosynthetic chromophores Chl-*a* and Per in PCP and molecular oxygen $O_2$. The diagram shows their interaction during the energy deactivation pathway.

Figure 2 shows the energy diagram of the photosynthetic chromophores Chl-*a* and Per (in PCP), their interaction and deactivation paths. For Chl-*a*, the ground state ($S_0$), the triplet state ($T_1$), the $S_1$ ($Q_y$ ), $S_2$ ($Q_x$) and the Soret transition are drawn. After promoting the Chl-*a* to its singlet excited state ($^1$Chl$^*$), a chlorophyll triplet is formed by inter system crossing (ISC). Chlorophyll triplet ($^3$[Chl]$^*$) is resonant with molecular oxygen ($^3$[O]$_2$) which is found in the ground state as triplet. Energy transfer (ET) from $^3$[Chl]$^*$ to $^3$[O]$_2$ can lead to promotion of $O_2$ to a singlet excited state configuration which is highly harmful for the organism.

## Carotenoids

Carotenoids are natural pigments that are to a significant extent responsible for the coloring of our surrounding world; fish and bird species as well as vegetables often owe their colors to carotenoids. In photosynthesis, carotenoids allow the photosynthetic organisms to absorb blue-green sunlight and transfer the electronic energy to (bacterio)chlorophyll molecules which do not absorb at these

wavelengths. In this way, these molecules make the blue-green light available for photosynthetic energy conversion; furthermore, carotenoids are not solely involved in light harvesting processes but perform other important functions like structure stabilization [7] and photoprotection [8, 9].

In many cases, the long polyene chains that form the carotenoids are essential for the structural stability of light-harvesting proteins; it has been shown that without carotenoids, such proteins will not fold or will disassemble if the carotenoids are removed [7].

In the photosynthetic apparatus, carotenoids are used for protection against photo-oxidation. Highly reactive singlet oxygen ($^1O_2^*$) can be formed, by triplet Excitation Energy Transfer (TEET), between (B)Chl triplet state ($^3$[(B)Chl]$^*$) and ground-state triplet oxygen ($^3[O]_2$):

$$^3(B)Chl^* + {}^3O_2 \rightarrow {}^1(B)Chl + {}^1O^*_2$$

Carotenoids can quench (B)Chl triplet states ($^3$[(B)Chl]$^*$) via their triplet excited state ($^3$[Car]$^*$):

$$^3(B)Chl^* + {}^1Car \rightarrow {}^1(B)Chl + {}^3Car^*$$

In addition, carotenoids can directly scavenge the singlet oxygen once it is formed:

$$^1O_2^* + {}^1Car \rightarrow {}^3O_2 + {}^3Car^*$$

Two particular carotenoids are studied and discussed in this thesis: Peridinin (Per) and 3' -hydroxy-echinenone (hECN). Per is present in the Peridinin-Chlorophyll-*a*-Protein (PCP) LH antenna as the main chromophore. hECN is found as the only pigment present in the Orange Carotenoid Protein, directly involved in photoprotection [10-15].

## Peridinin (Per)

The absorption spectrum of Per measured at room temperature is shown in Figure 3 the Per absorption in solution appears between 350-600 nm with peaks at 485 nm and 455nm with a shoulder at 428 nm in n-hexane.

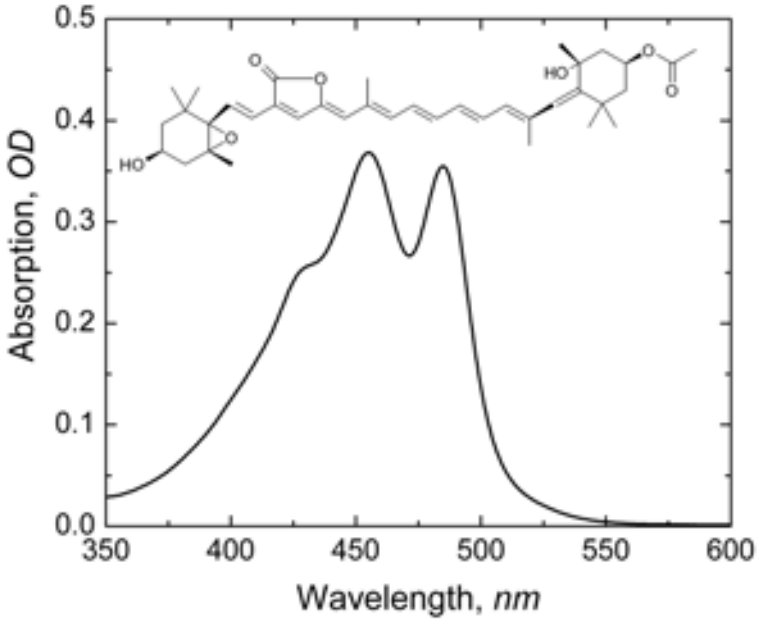


**Figure 3**: Absorption spectrum of Peridinin in n-hexane and structural formula.

Peridinin is the most highly substituted Car known in nature, it has an unusually short carbon skeleton ($C_{37}$), an allene group and a lactone ring both conjugated with the backbone (see insert in Figure 3). At both ends of the conjugated carbon chain, two β-rings are located with an epoxy group with a secondary alcohol group, and an ester group located on the opposite β-ring with a tertiary alcohol group.

## Light-Harvesting Complexes

### The Peridinin-Chlorophyll-a-Protein (PCP)

One of the most interesting oceanic photosynthetic algae belongs to the family of *dinoflagellates*; this eukaryotic algae uses a water-soluble Peridinin-chlorophyll-protein (PCP) as LH antenna with an unusual Chl-*a* : Per stoichiometry of 1:4. In vivo, PCP is found as a trimer, it harvests sunlight and transfers energy to the photosystem II (PSII) reaction center (RC). The structure of PCP obtained at 2 Å resolution [16, 17], revealed that each monomer (in Figure 4) is divided into two quasi-symmetric subunits containing a Chl-*a* closely surrounded by four Per

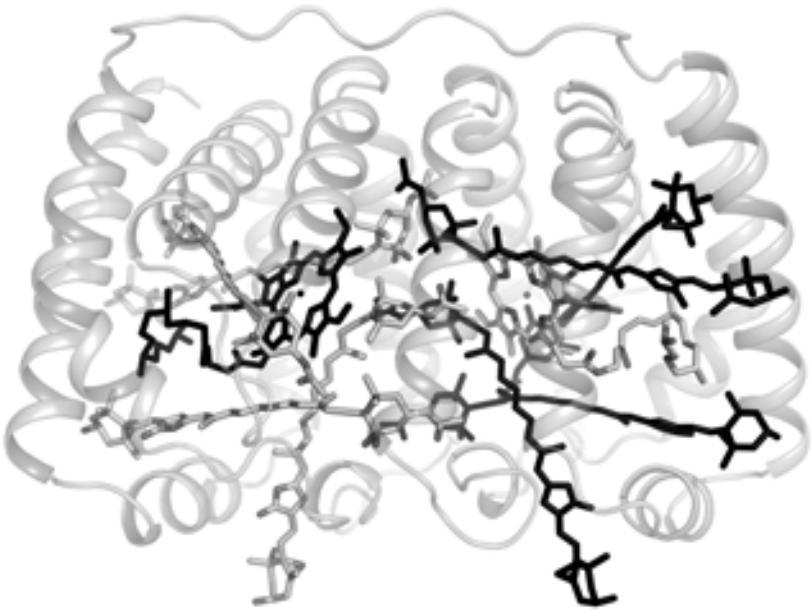

**Figure 4**: Structure of the light-harvesting complex Peridinin-Chlorophyll-*a* Protein (PCP). The chromophores are shown in black and gray, the α-helices of the protein are represented as coiled ribbons. Panel prepared with PYMOL (DeLano, W.L. (2002) The PyMOL Molecular Graphics System, www.pymol.org).

molecules. Peridinins are excellent light harvesters, they have a strong absorption in the green from 480 to 530 nm when bound to PCP and achieve a high efficiency of excitation energy transfer (EET) to Chl-*a* (of ~90%) which is proposed to result from the tight packing of the pigments as well as the peculiar excited state manifold of peridinin [18-20]. This chromophore organization is also responsible for the efficient Chl-*a* triplet quenching of 100% [18, 21, 22].

## Photoreceptors

Photoreceptors are proteins functioning as sensors of light signals used by organisms to monitor their light environment and to respond to the changes. These proteins allow them to protect themselves from potential harmful UV light, or to adjust growth and developments optimize the available light conditions. Dependent upon the environment, nature has selected a small variety of chromophores used by the photoreceptors to cover a broad spectral range. Once the co-factor is photo-excited its electronic configuration changes, initiating a chain reaction of events that

ends with a transient change in the tertiary or quarternary structure of the photoreceptor-protein. This change "travels" from the chromophore-binding pocket across the protein reaching the protein surface. There the light-induced meta-stable state (signalling state) transfers the information of light-absorption to a partner in the signal transduction pathway. At the end of the process, the organism will respond to the light absorption changing, for instance via gene-expression or speed or direction of movement.

To date, only six well established photoreceptor families are known: rhodopsin, xanthophsin, phytochromes, cryptochromes, LOV and BLUF proteins. Rhodopsin, xanthophsin and phytochromes, although they bind different chromophores (retinal, p-coumaric acid and linear tetrapyrrole, respectively), have the same activation mechanism: light-induced E/Z isomerization around a particular double bond in their co-factor [23]. Conversely, cryptochromes, LOV and BLUF share the same chromophore, flavin, but their light-activation mechanisms are very different. In cryptochromes the mechanism of activation is presumably electron transfer [23], in LOV it is the transient formation of a covalent adduct [23]. In BLUF proteins the signal transduction follows the reorganization of an H-bond network between co-factor and side chain residues because of transient H transfer, with the consequent flipping of a highly conserved Glutamine [23-26].

Recently OCP, a protein present in cyanobacteria and containing 3' -hydroxy-echinenone, has been characterized as another photoreceptor, opening a new area of investigation.

## BLUF domain proteins

The blue-light photoreceptor family using flavin as their co-factor, is the so called BLUF domain family. Only a few years ago, the study of the blue-light sensitivity of photosynthetic gene expression in *Rhodobacter sphaeroides*, brought the discovery of this class of photoreceptors, called BLUF from "sensor of Blue-Light Using Flavin" [27].

The first BLUF protein that was discovered and characterized was AppA (from *Rhodobacter sp.*); the last few years BLUF domains have been the object of intensive research aimed at elucidating the mechanism

of photoactivation. In the mean time the BLUF family has been enriched with many additional members.

The structure of a BLUF domains shows five β-strandss and two α-helixes (βαββαββ topology) that sandwich the flavin chromophore (see Figure 5). Upon illumination with blue light, BLUF domains show a characteristic spectral red-shift of their absorption spectrum by approximately 10 nm, which is thought to correspond to the signaling state [28]. Vibrational spectroscopy has indicated that a light-induced hydrogen-bond rearrangement among FAD and nearby amino acid side-chains underlies BLUF photoactivation [29-31]. Binding pocket configurations for the Dark and Light states were initially proposed for AppA [24]. In the relaxed state (Dark State) the binding pocket has the flavin involved in a H-bond network with the nearest residues (Figure 6) Y8 and Q50; upon light absorption the H-bonding-network is reorganized with flipping of the glutamine (Q63) and consequently signalling state formation (Light State). However, the photochemistry involved in the light-activation has been revealed only recently by applying UV/visible ultrafast time-resolved spectroscopy on another member of the BLUF domain family, Slr1694 from *Synechocystis sp.* PCC6803 [26]. The capability of the isoalloxazine system to undergo reversible oxidation and reduction allows the formation of two intermediate configurations that leads to the Light State (Figure 7) . The flavin assumes first the anion and later the neutral semiquinone redox configuration. These states appear due to the interaction with the electron and proton donor Y8 (homologue of Y21 for AppA) . The involvement of Y8 and Q50 (homologue of Q63 for AppA) and the role played by other side chain residues (W91 and S28) in the photo-activation have been investigated by mid-IR and UV/visible femtosecond time-resolved spectroscopy, and will be discussed in more detail in Chapter 5 and Chapter 6.

**Figure 5**: Three-dimensional structure of the *Synechocystis* Slr1694 BLUF domain. The only chromophore, FAD, is shown in gray shadows; the β-sheets and α-helices of the protein are represented as flat and coiled ribbons, respectively. Panel prepared with PYMOL (DeLano, W.L. (2002) The PyMOL Molecular Graphics System, www.pymol.org)

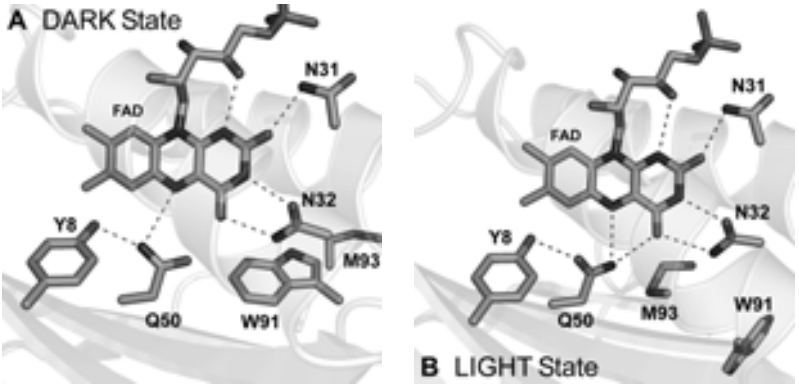


**Figure 6**: X-ray structure of the *Synechocystis* Slr1694 BLUF domain with the hydrogen bond patterns lining the FAD binding pocket in proposed dark state (A) and light state (B) configurations. Panels A and B prepared with PYMOL (DeLano, W.L. (2002) The PyMOL Molecular Graphics System, www.pymol.org)

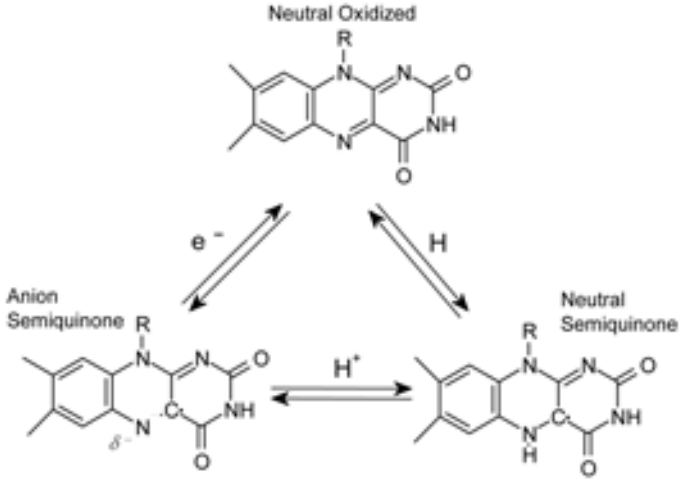


**Figure 7**: The scheme in the figure represents different radical configurations, i.e., neutral oxidized, anion semiquinone (oxidized one-electron reduced) and neutral semiquinone (oxidized one-electron reduced and protonated). Inside the protein, the capability of flavin to undergo reversible oxidation and reduction allows the formation of two intermediate configurations that lead

## Orange-Carotenoid-Protein from the cyanobacterium Arthrospira maxima: OCP

Photosynthetic organisms have developed processes to protect themselves from excess light. These mechanisms go under the generic name of Non Photochemical Quenching (NPQ). Thermal dissipation of the excess of excitation energy is one of those processes that take place in the antenna of Photosystem II (PS II) to diminish the energy arriving to the reaction centre and avoid irreversible damage. Recently, NPQ mechanisms were described in cyanobacteria[10, 11, 13-15, 32], photosynthetic organisms in which photoprotection mechanisms were previously believed to be absent. Wilson et al. demonstrated that OCP, a soluble orange-carotenoid-protein, and the phycobilisomes, the extra-membranal antenna of PS II in cyanobacteria, are essential for this mechanism [13]. The soluble orange-carotenoid-protein (OCP) is a 35 kDa protein that contains a single non-covalently bound carotenoid [33-36]. The structure of the *Arthrospira maxima* OCP has been determined to 2.1 Å resolution [37]. Figure 8 shows the crystal structure of OCP with its two domains: an all α-helical N-terminal domain and a mixed α/β C-terminal domain. Spanning from the C- to N-terminal is a carotenoid, 3' -hydroxy-echinenone (hECN), in all-*trans* configuration. The hECN (Figure 8) has a conjugated carbonyl group located at the terminus of a conjugated chain of 11 C=C bonds, forming H-bridges with

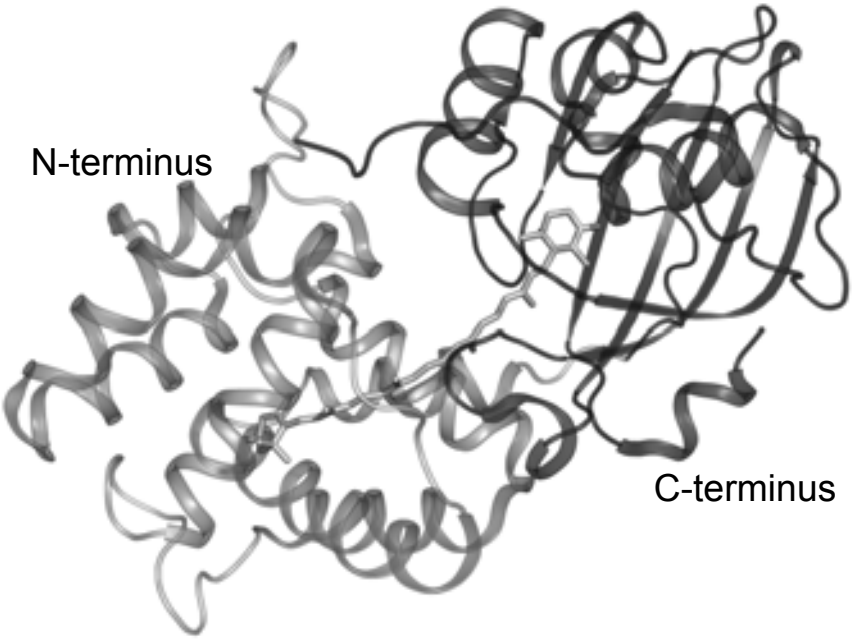


**Figure 8**: View of the OCP X-ray structure. The N-terminus is shown in light gray, the C-terminus in dark gray. The hECN molecule is displayed in gray shadows. The β-sheets and α-helices of the protein are represented as flat and coiled ribbons, respectively. Panel prepared with PYMOL (DeLano, W.L. (2002) The PyMOL Molecular Graphics System, www.pymol.org)

Y203 and W290 residues [37]. In the binding protein, hECN absorbs maximally between 400 and 500 nm with the main peaks at 470 nm and 496 nm and shoulder at 436 nm (black spectrum in Figure 9), conferring to the protein a bright orange color. Upon illumination with blue-green light (400-550nm) the orange OCP is photoconverted to a red OCP. The associated spectrum, in gray in Figure 9, shows a red-shift of the absorption to 507 nm and loss of the vibronic structure present in the steady state absorption of the orange form. In Chapter 4 we show that OCP is a photoactive protein that, upon blue light excitation forms a signalling state (see also dashed spectrum in Figure 9). OCP is the first example of a photoactive protein with a carotenoid as the photoactive chromophore although retinal is often referred to as a half carotenoid.

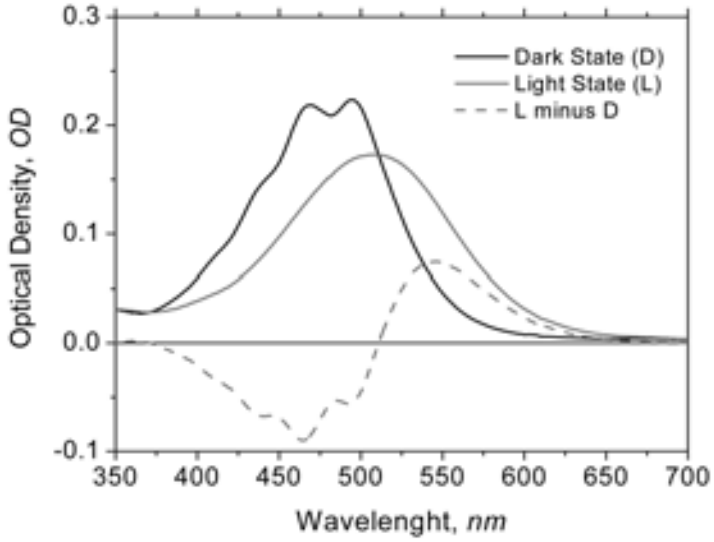


**Figure 9**: Absorption spectra in buffer (aqueous) of the orange form (dark state, black line) and red form (light state, gray line) of OCP. Dashed line difference the light minus dark spectrum.

## Techniques, Tools and Methods

As already mentioned, the aim of this thesis is to investigate the primary reactions that take place in photo-active proteins or chromophores after illumination. The processes that follow immediately after the light excitation, take place on the time scale of femtoseconds to picoseconds and require an ultra-fast apparatus to be adequately recorded. Femtosecond titanium:sapphire (Ti:S) lasers provide the ideal tool to the experimentalists to trigger the photochemistry in proteins and chromophores and follow their time evolution.

### Pump-Probe Spectroscopy

Transient absorption spectroscopy, more commonly named Pump-Probe spectroscopy, is the widest used technique to monitor changes of the optical properties of a sample in time. The absorbance or optical density (OD) of a sample at a certain wavelength ($\lambda$) or wavenumber ($\nu$) is defined by:

$$OD(\vartheta) = -\log((I(\vartheta))/(I_0(\vartheta))),\ \vartheta = \lambda or \nu$$

where $I_0(\theta)$, is the incident light intensity, and $I(\theta)$, the light intensity transmitted by the sample, are experimental quantities. Knowing the OD as a function of λ (the color of the light) or ν (the energy of the light) means to know the spectrum of the sample.

In transient absorption measurements, the photochemistry of the sample is triggered by an intense laser pulse (pump) chosen to be resonant with an electronic transition of one of the chromophores in the sample. A second pulse, weaker than the pump and polychromatic (probe), is administered on the sample after the pump (delay). The change in the absorption of the probe light, ΔOD, induced by the pump is recoded as function of the time delay between pump and probe:

$$\Delta OD(\lambda, t) = OD(\lambda, t)_{on} - OD(\lambda)_{off} = \log \frac{I(\lambda)_{off}}{I(\lambda, t)_{on}}$$

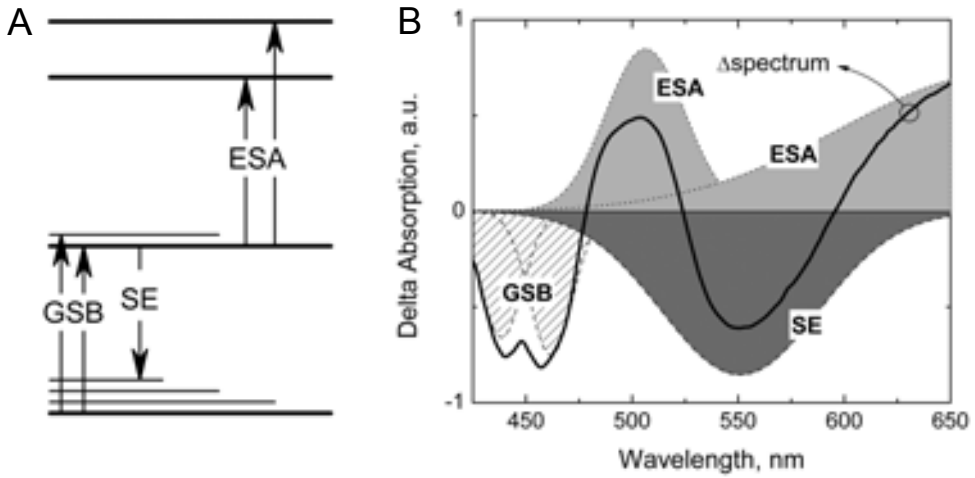


Figure 10: A, the energy level scheme of a molecule and the processes observed in the UV/Visible pump and probe experiments. B, ground state bleaching (GSB) stimulated emission (SE) and excited state absorption (ESA) are superimpose forming of the final pump-probe spectrum.

The difference spectrum is obtained comparing at each delay time two absorption spectra, with and without the pump pulse, of the probe light in the sample. The resulting difference absorption (ΔOD) spectrum will contain negative and positive bands, reflecting the original ground state (bleaches), S.E. and products. Using a mid-IR probe pulse we probe the vibrational modes associated with the electronic transitions of the ground state (bleaches) and product (bands appearing) (see Figure 10).

In Chapters 2, 4, 5 and 6, we will present results obtained using the pump-probe technique with a visible-pump and a UV/visible (Chapters 4 and 6) or a mid-infrared (Chapters 2 and 5) probe.

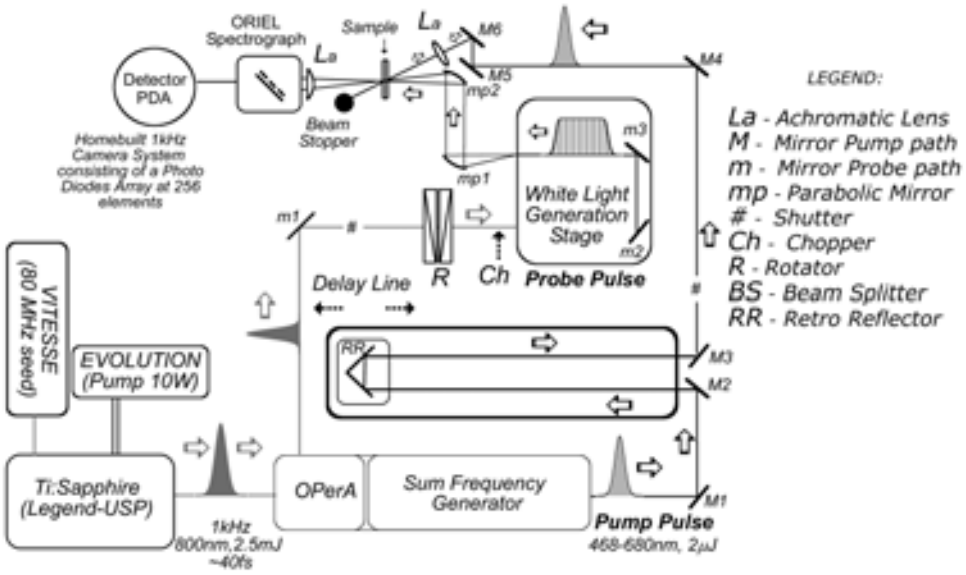


**Figure 11**: Schematic representation of the ultra-fast time-resolved Visible pump UV/Visible probe experimental set-up used to collect the data presented in this thesis in Chapters 4 and 6. A detailed description is given in the text.

## Femtosecond time-resolved UV/visible-pump and probe setup

Time-resolved measurements presented in Chapters 4 and 6 were performed on a visible-pump, visible-probe setup. The system, shown in Figure 11, uses a Coherent Legend-USP Ti:S amplifier oscillator (1kHz),

providing a light source with a central wavelength of 800nm, bandwidth of ~50 nm at FWHM, with an average energy of 2.5 mJ/pulse and a duration of ~40 fs. The 800 nm pulse is split in two parts: one part is used to drive an optical parametric amplifier (Coherent OPerA) able to generate light from 468 nm up to 680 nm with an output energy of 2μJ per pulse, which triggers the photo reaction; the remaining fraction of the fundamental 800 nm, is focused on a rotating $CaF_2$ crystal to generate a white-light continuum, needed to probe the sample. The polarization between pump and probe beams was set to magic angle (54.7 ° ). The probe pulse is focused on the sample by parabolic mirrors to avoid chromatic aberration; for the same reason an achromatic lens (fl:200 mm) is used to focus the pump pulse. The pump pulse is progressively delayed with respect to the probe using a 60-cm long delay stage (Newport IMS-6000) to cover a time window up to 3.7 ns. The sample, placed in a quartz flow cell of 2 mm optical path, is fixed in the focal plane of the two focusing elements (achromatic lens and parabolic mirror) and circulated by a peristaltic pump. After the sample, the pump, and probe beams are spatially separated. Only the probe beam is collimated in a spectrograph (Oriel) and spectrally dispersed across a homebuilt photo-diode array. This 256-pixel array is read out and the data are parsed to a computer to calculate the optical densities. Out of the thousand pulses per second, 500 pump-pulses are blocked by a chopper, synchronized with the Ti:S laser, to allow to measure the difference in absorption of the white light between molecules pumped and non-pumped.

## Femtosecond time-resolved visible-pump mid-IR-probe setup

The experimental setup used for the measurements of PCP and Slr1694 wild type, presented in Chapter 2 and Chapter 5, is shown in Figure 12. It consists of a regeneratively amplified Ti:S laser system (Hurricane, Spectra Physics Inc.) providing a 800 nm source, with a maximum output of 0.8 mJ, repetition rate at 1 kHz and pulse duration between 80 and 90 fs. Using a beamsplitter, a portion of the 800 nm source is used to pump a tunable optical parametric generator and amplifier with a difference frequency generator (TOPAS, Light Conversion, Vilnius, Lithuania) able to produce a mid-IR output (tunable between 2.4 and 11 μm) with a bandwidth of ~ 200 $cm^{-1}$ and energy between 5 and 15 μJ. The probe

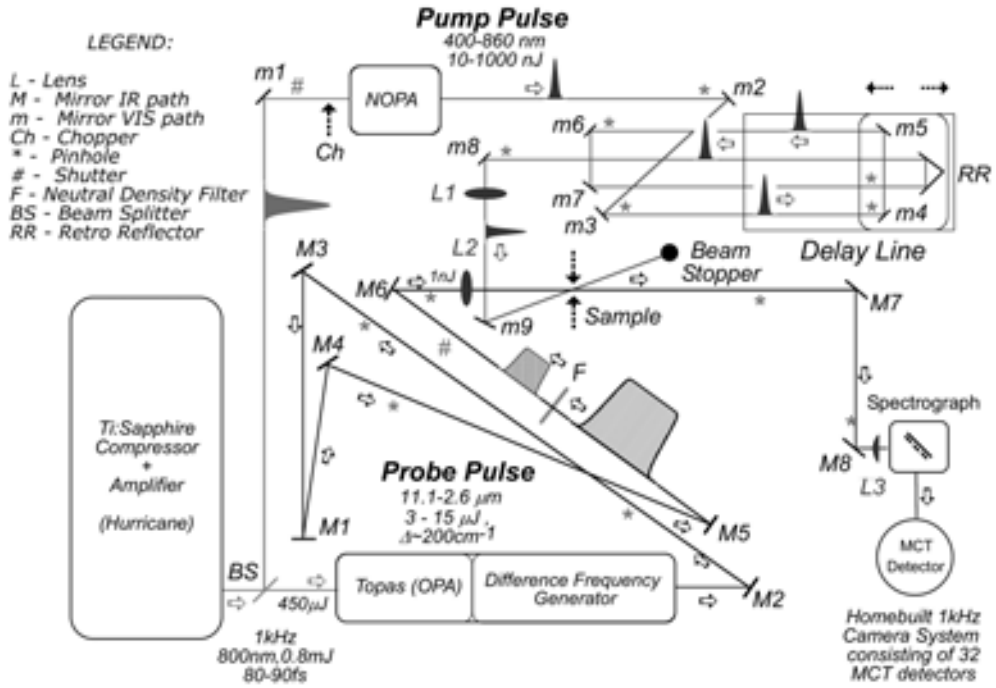


Figure 12: Schematic representation of the ultra-fast time-resolved Visible pump mid-IR probe experimental set-up used to collect the data presented in this thesis in the Chapter 2 and 5. See text for details.

pulse on the sample is attenuated to 1 nJ using neutral density filters (symbolized by the F filter in Figure 12). The remaining part of the 800 nm light is sent into a home-built non-collinear optical parametric amplifier (NOPA) which is used to trigger the photoreaction in the sample, and progressively delayed by a 60-cm long delay stage (Newport IMS-6000) to cover a time window of 3ns (Chapter 5, Figure 12) up to 6 ns (Chapter 2, Figure 13) . The pump pulse can be tuned to produce 60 fs excitation pulses with a wavelength range of 475 – 800 nm and energy between 100 and 500 nJ (per pulse). The probe has a diameter of about 120–150 μm, the pump is the same size or slightly larger. After the sample the probe is collimated into the entrance of a spectrograph (Chromex) and dispersed by it onto a 32 – element Mercury Cadmium Tellurium detector (MCT, Infrared Associates). The Chromex can use three different internal gratings with 150, 75, or 50 grooves per mm, yielding a maximal spectral resolution of 4 $cm^{-1}$. All 32 channels are individually amplified, and read out by 32 home – built integrate – and – hold (IH) devices. A PC with a

data – acquisition card (PCI6031E, National Instruments) is used to collect and record the signals from the IH – box.

The infrared probe path is entirely placed inside a nitrogen gas or dry air purged box to reduce absorption due to water vapor. A phase – locked chopper (500 Hz) blocks every other pump – laser shot, so that the transmission with and without pump can be recorded. In this way the pump – induced change in transmission can be determined and the difference absorption can be calculated.

With the above described experimental set-up it is possible to perform measurements of sample anisotropy using a Berek rotator (Model 5540; New Focus, San Jose, CA) to set different polarization for the two pump and probe pulses. However, to perform anisotropy – free measurements the polarization between pump and probe is set at 54.7 ° .

The sample is placed in a sample cell formed by two $CaF_2$ plates separated by Teflon rings of different thickness to have control on the optical path of the pump and probe pulse into the sample. To avoid multiple laser shots on the same volume during the measurements, the sample is moved by a home-built Lissajous scanner. To obtain spatial and temporal overlap of the visible and mid – IR beam a 50 μm thick slab of GaAs is used. The visible excitation pulse creates free carriers in this semiconductor which results in a large change in the index of refraction. Thus huge changes in the transmission of the IR pulse are easily measured because they correspond to several hundreds of mOD of absorption change. Maximization of the mid-IR absorption in GaAs allows precise determination of the overlap of pump and probe in both space and time. Using this absorption in GaAs it is possible to measure the cross correlation of the visible and IR pulses: a value of 180 fs was obtained.

## Increasing the time window

Ultrafast mid-IR and step scan time-resolved Fourier transformed infrared (FTIR) spectroscopy are complementary techniques to observe the dynamics of relaxation after photoexcitation. Jointly they can cover the from the femtosecond to millisecond time scale. Femto-IR spectroscopy covers the first few nanoseconds of the photochemistry when most of the action happens inside the chromophore binding pocket, involving co-factor and the neighboring amino acid residues. Instead, with step scan FTIR spectroscopy it is possible to observe dynamic

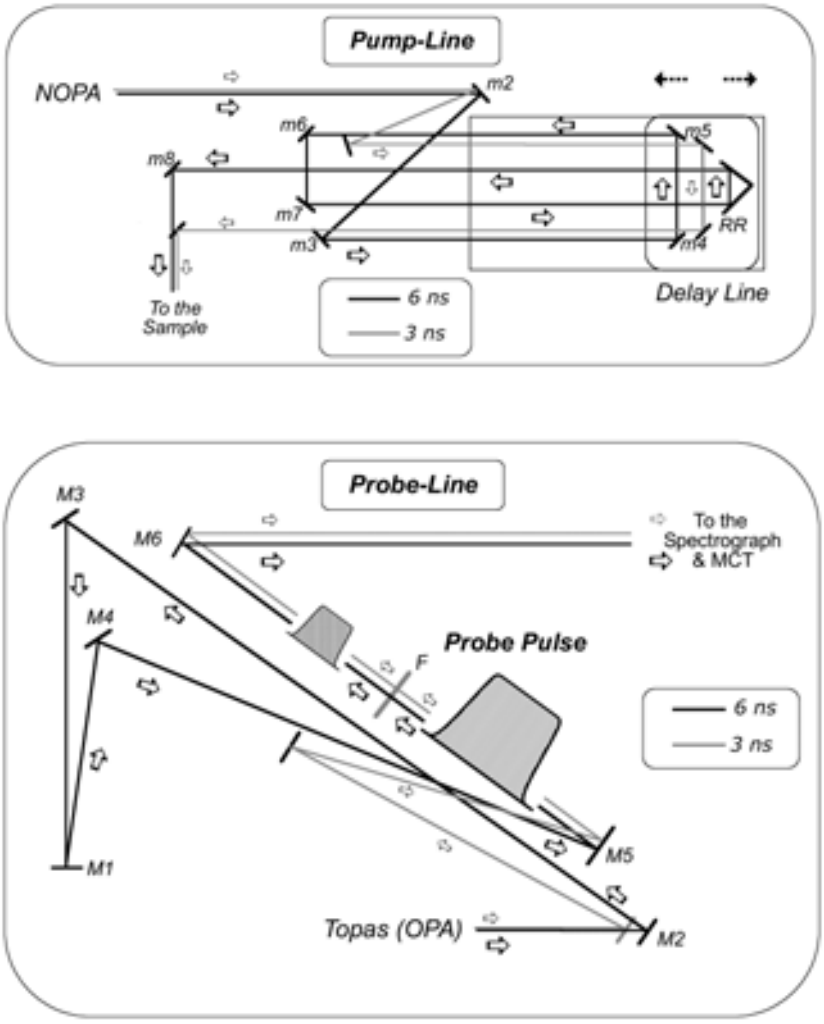


**Figure 13**: In Chapters 2 and 5 the maximum delay between pump and probe beams was set differently. In the figure we shown the two different configurations for : **A**, pump-line; **B**, probe-line used for the ultra-fast time-resolved Visible pump mid-IR probe experimental set-up in Chapter 2 (6 ns delay, black paths) and Chapter 5 (3 ns delay, gray paths).

phenomena in a time scale from nano- to milliseconds. This extended time of observation allows the experimentalist to follow and characterize long lived species (i.e. triplets or radicals) or follow large-scale protein motions.

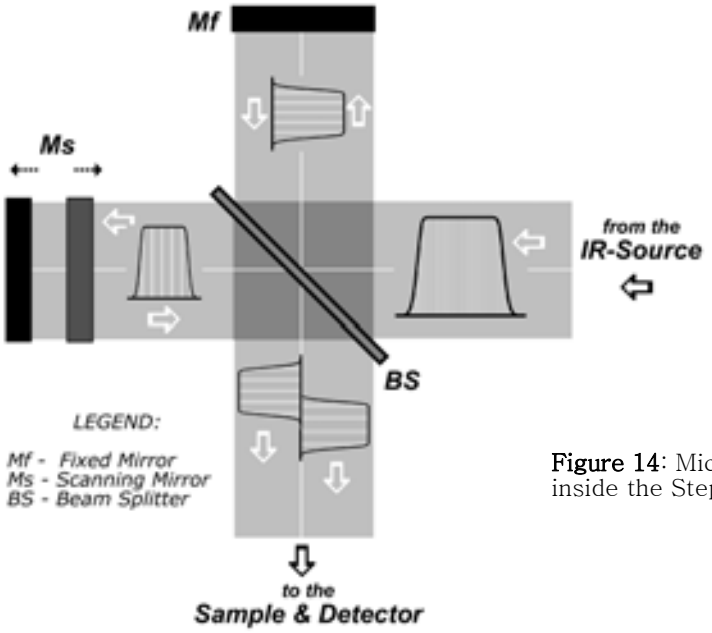


Figure 14: Michelson Interferometer inside the Step Scan system.

## Step Scan time-resolved FTIR spectroscopy

In contrast to the previously described dispersive IR spectroscopy technique (fs-IR), step scan FTIR is an interferometric method. This means that the spectrum is obtained after Fourier transformation of the interferogram. The philosophy of the step scan measurement is the following: an IR continuous beam is sent in the two harms of the interferometer (see Figure 14) and recombined on the IR-detector. The scanning mirror (Ms in Figure 14) is moved step by step around an equilibrium position $x_0$ for which the length of the two arms are equal. A software record the time dependent intensity of the IR-light on the detector at a given mirror position. For each mirror position, the protein activity in initiated (by a laser flash) and the time dependent IR signal on the detector is recorded for a given time. Then the Ms mirror "steps" to the next interferogram position, laser flash trigs the photoreaction and the time dependent IR signal is read by the detector. The process is reiterated at each sampling position of the interferogram. Once the interferogram is recorded, it is Fourier transformed to give the IR-absorption spectrum of the sample for a certain delay between pump and IR-light.

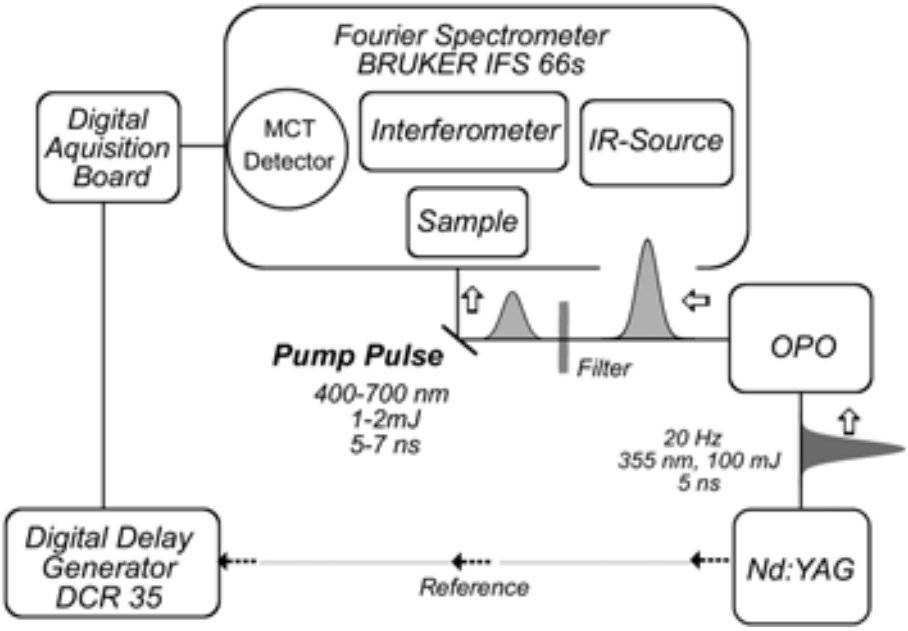


Figure 15: Schematic representation of the Step Scan time-resolved set-up used to collect the data presented in this thesis in Chapter 5. A detailed description of it is given in the text.

The experimental step scan set-up used in this thesis (Chapters 3 and 4) is shown Figure 15. A commercial step-scan FTIR spectrometer (IFS 66s Bruker) is placed in an acoustically isolated box and placed on an air-bearing table (Kinetic Systems) to improve the stability of the moving mirror in the Michelson interferometer (~4 nm precision). The spectrometer is purged with $N_2$ gas to reduce IR absorption by water vapor. The system is equippeded with a pre-amplified photovoltaic MCT detector (20 MHz, KV 100, Kolmar Technologies). The IR light impinging on the sample is filtered to block the laser light before the interferometer and the detector. The detector signal is recorded with the internal digitizer (200 kHz, 16-bit A/D converter) allowing a time resolution of 5 μs. A 20 Hz, Nd:YAG laser (5 ns, 100 mJ at 355 nm, Continuum) was used to pump an optical parametric oscillator (Panther, Continuum), producing tunable visible light from 400-700 nm, with a pulse duration of 5-7 ns. The obtained pump beam is filtered by a neutral density filter to set the energy delivered to the sample (usually 1-2 mJ) and weakly focused to a spot of 4 mm in diameter overlapping the slightly smaller IR

beam. A Stanford Research Systems digital delay generator (DCR 35) is used to vary the time delay between the laser pump pulse and the trigger of the detection electronics.

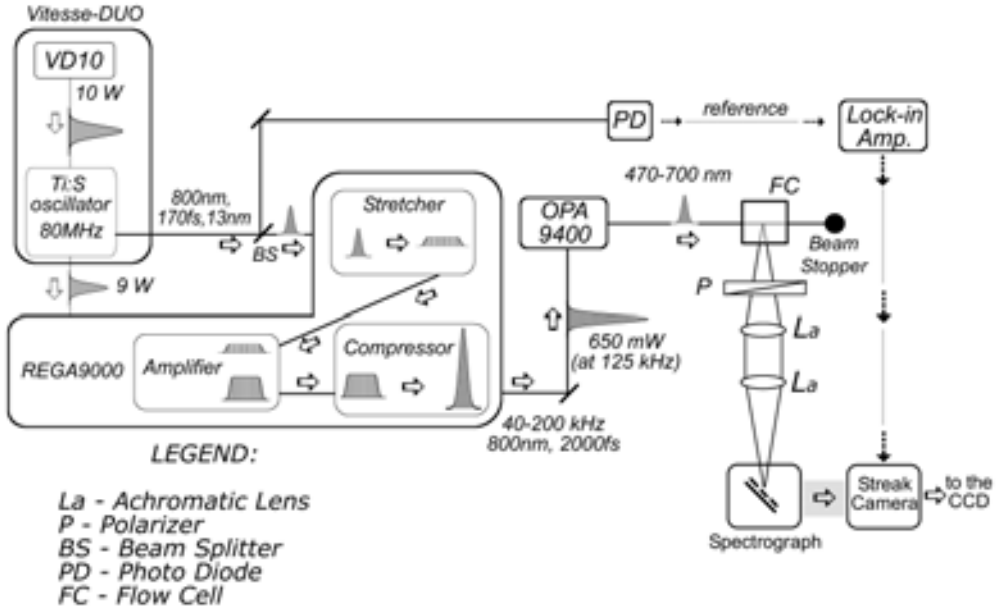


**Figure 16**: Schematic representation of the time-resolved fluorescence set-up. See text for details.

## Time-Resolved Fluorescence: synchroscan streak camera

Time-resolved fluorescence measurements are employed in Chapter 4, for which a synchroscan streak camera system (Figure 16) was used. Inside a Vitesse-Duo (Coherent Laser Group, Santa Clara, California USA) ~10% of the 10W Verdi laser (VD10) is used to pump the 80 MHz Vitesse-Duo Ti:S oscillator. The output power of the oscillator is ~140 mW, pulse duration of 240 fs autocorrelation (so 170 fs), central wavelength at 800nm, bandwidth 13 nm. The rest of the output of the VD10 (about 9 W) is used to pump the Rega 9000 (also from Coherent Laser Group). Here, the output from the Ti:S oscillator is stretched in time amplified and compressed to reach a pulse duration of 280 fs autocorrelation (about 200 fs) and a repetition rate variable between 40 and 200 kHz. At 125 kHz the (compressed) power out of the Rega 9000 is typical 650 mW. This output is directed inside the OPA9400 (Coherent

Laser Group) which produces a tunable output between 470 and 700 nm. The pulses of the selected color are focused into the sample, which is contained in a quartz flow cell of 1 mm path length (FC). Fluorescence is collected through a sheet polarizer (P) set at the magic angle (54.7 ° ) at 90 ° with respect to the excitation (see Figure 16), and focused into a spectrograph (S-Chromex 250IS) using two triplet achromatic lenses (La). The output of the spectrograph is focused onto the entrance slit of the Hamamatsu C5680 synchroscan streak camera and recorded on a Hamamatsu C4880 CCD camera, cooled to -55 ° C.

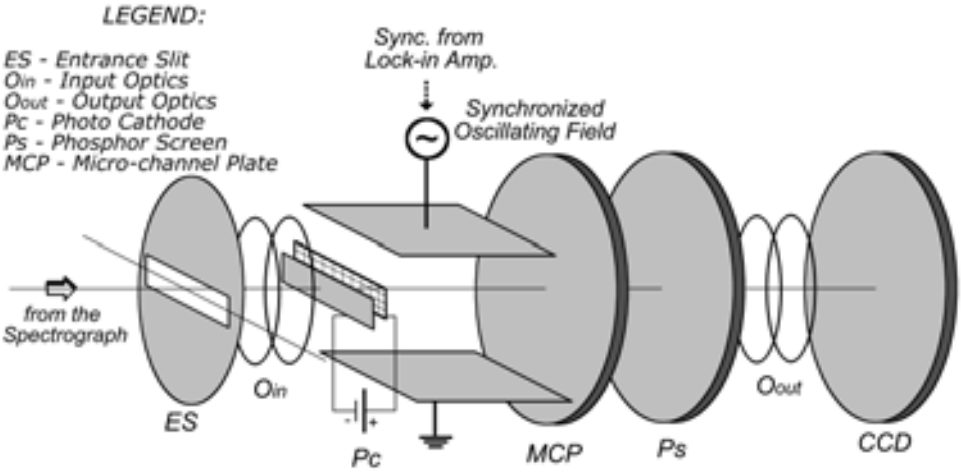


**Figure 17**: Schematic representation of a synchroscan streak camera. A detailed description is given in the text.

The streak camera is the heart of the time-resolved fluorescence measurement set-up; a schematic representation is given in Figure 17. The fluorescent photons are dispersed by a spectrograph and enter the system through a horizontal entrance slit (ES in Figure 17) which is imaged, by internal input optics ($O_{in}$) onto a photocathode ($P_c$). Here, a number of electrons are released proportional to the intensity of the incident light. These electrons are first linearly accelerated and subsequently vertically deflected by an oscillating electric field, resulting in a time dependent vertical deflection of the electrons. The electron flow is amplified in a microchannel plate (MCP) and re-converted into monochromatic photons on a phosphor screen ($P_S$), subsequently recorded with a high-sensitivity CCD camera. The oscillating field must be synchronised with the repetition rate of the laser, such that the signal

of a large number of successive laser pulses (synchroscan) can be accumulated on the CCD camera. The resulting "streak image", (Figure A in the *Appendix* of Chapter 5) represents the fluorescence intensity as a function of both wavelength and time.

## Data Analysis

The time-resolved measurement techniques described above produce, as output, a dataset in which changes in detected intensity are measured as a function of time and wavelength. To correlate different wavelength – regions and time scales it is necessary to analyze all acquired data simultaneously. This kind of analysis technique is called *Global Analysis* [38]. The aim of global analysis is to mathematically describe the observed signal $S$ at any given time ($t$) or wavenumber ($\lambda$) and extract and quantify physical information out of the immense amount of data. The description of $S$ should be obtained with a minimum amount ($i$) of time constants ($k_i$) that result in a good quality of fit. The total dataset is a superposition of contributions from different species (components) having their own time constants (lifetime). Each component starts with a given concentration ($c_i$) that decays in time and possesses its own specific time – independent spectrum ($\varepsilon_i$):

$$S(\upsilon, t) = \sum_{i=1}^{n} c_i(t) * \varepsilon_i(\upsilon)$$

$$with \qquad c_i = e^{(-k_i t)}$$

However, the experimentalist must be aware of the fact that $\varepsilon_i$, the resulting spectra, do not always contain physically relevant information. In this sense, information obtained using different experimental techniques, or previous knowledge of a system such as an already (partially) defined protein photocycle, can be helpful in such a context. At the end, the simplest model describing the measured data has to be chosen (*lex parsimoniae* or Ockham' s razor). Possible model templates are: the sequential and parallel models (see Figure 18A and B), where one compartment decays monoexponentially into the next one or towards the ground state (Figure 18B) or a branched model (Figure 18C), a more

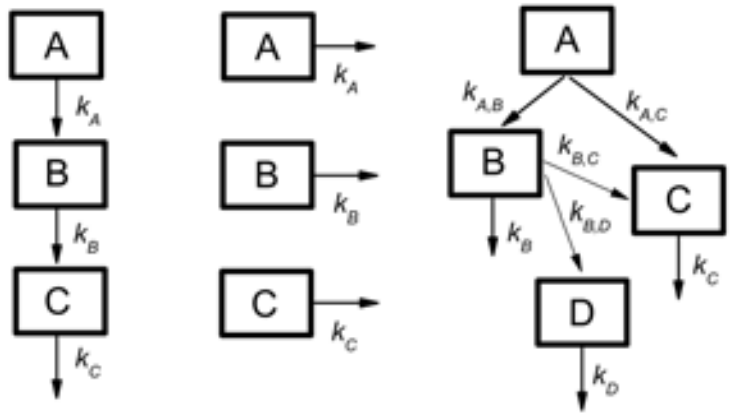


**Figure 18**: Typical kinetic schemes used for global analysis: **A**, Sequential model; **B**, Parallel model; **C**, Branched model.

complicated model where one compartment can populate two other compartments.

More details on the data analysis can be found in the following chapters and, in particular, in the supporting information of Chapter 5.

## References

1. Barber J: **The Photosystems: Structure, Function and Molecular Biology**. Amsterdam: Elsevier; 1992.
2. Blankenship RE: **Molecular Mechanisms of Photosynthesis**. Malden, Massachusetts: Blackwell Science; 2002.
3. Brody SS, Rabinowitch E: **Excitation lifetime of photosynthetic pigments in vitro and in vivo**. *Science (New York, NY* 1957, **125**(3247):555.
4. van Amerongen H, Valkunas L, van Grondelle R: **Photosynthetic Excitons**. Singapore: World Scientific; 2000.
5. Scheer H: **Chlorophylls**. Boca Raton, Florida: CRC Press; 1991.
6. Stryer L: **Biochemistry**. New York: W.H. Freeman and Company; 1995.
7. Frank HA, Cogdell RJ: **Carotenoids in photosynthesis**. *Photochem Photobiol* 1996, **63**(3):257–264.
8. Govindjee R: **Carotenoids in Photosynthesis: An Historical Perspective**. In: *The Photochemistry of Carotenoids.* Edited by

Frank HA, Young AJ, Britton G, Cogdell RJ. Dordrecht: Kluwer Academic Publishers; 1999: 1-19.

9. Krinsky NI: **Function**. In: *Carotenoids.* Edited by Isler O, Guttmman G, Solms U. Basel: Birkhauser Verlag; 1971: 669-716.
10. Rakhimberdieva MG, Bolychevtseva YV, Elanskaya IV, Karapetyan NV: **Protein-protein interactions in carotenoid triggered quenching of phycobilisome fluorescence in Synechocystis sp. PCC 6803**. *FEBS Lett* 2007, **581**(13):2429-2433.
11. Rakhimberdieva MG, Stadnichuk IN, Elanskaya IV, Karapetyan NV: **Carotenoid-induced quenching of the phycobilisome fluorescence in photosystem II-deficient mutant of Synechocystis sp**. *FEBS Lett* 2004, **574**(1-3):85-88.
12. Rakhimberdieva MG, Vavilin DV, Vermaas WF, Elanskaya IV, Karapetyan NV: **Phycobilin/chlorophyll excitation equilibration upon carotenoid-induced non-photochemical fluorescence quenching in phycobilisomes of the cyanobacterium Synechocystis sp. PCC 6803**. *Biochim Biophys Acta* 2007, **1767**(6):757-765.
13. Wilson A, Ajlani G, Verbavatz JM, Vass I, Kerfeld CA, Kirilovsky D: **A soluble carotenoid protein involved in phycobilisome-related energy dissipation in cyanobacteria**. *The Plant cell* 2006, **18**(4):992-1007.
14. Wilson A, Boulay C, Wilde A, Kerfeld CA, Kirilovsky D: **Light-induced energy dissipation in iron-starved cyanobacteria: roles of OCP and IsiA proteins**. *The Plant cell* 2007, **19**(2):656-672.
15. Wilson A, Punginelli C, Gall A, Bonetti C, Alexandre M, Routaboul JM, Kerfeld CA, van Grondelle R, Robert B, Kennis JT *et al*: **A photoactive carotenoid protein acting as light intensity sensor**. *Proc Natl Acad Sci U S A* 2008, **105**(33):12075-12080.
16. Hofmann E: **Strukturanalyse der Lichtsammler Peridinin-Chlorophyll a-Proteine (PCPs) von Amphidinium carterae und Heterocapsa pygmaea**. 1999.
17. Hofmann E, Wrench PM, Sharples FP, Hiller RG, Welte W, Diederichs K: **Structural basis of light harvesting by carotenoids: peridinin-chlorophyll-protein from Amphidinium carterae**. *Science* 1996, **272**(5269):1788-1791.
18. Bautista JA, Hiller RG, Sharples FP, Gosztola D, Wasielewski M, Frank HA: **Singlet and triplet energy transfer in the peridinin-chlorophyll a protein from Amphidinium carterae**. *Journal of Physical Chemistry A* 1999, **103**(14):2267-2273.
19. Krueger BP, Lampoura SS, van Stokkum IHM, Papagiannakis E, Salverda JM, Gradinaru CC, Rutkauskas D, Hiller RG, van Grondelle R: **Energy transfer in the peridinin chlorophyll-a protein of**

Amphidinium carterae studied by polarized transient absorption and target analysis. *Biophys J* 2001, **80**(6):2843-2855.

20. Song PS, Koka P, Prezelin BB, Haxo FT: **Molecular topology of the photosynthetic light-harvesting pigment complex, peridinin-chlorophyll a-protein, from marine dinoflagellates.** *Biochemistry* 1976, **15**(20):4422-4427.
21. Kleima FJ, Hofmann E, Gobets B, van Stokkum IHM, van Grondelle R, Diederichs K, van Amerongen H: **Forster excitation energy transfer in peridinin-chlorophyll-a-protein.** *Biophysical Journal* 2000, **78**(1):344-353.
22. Kleima FJ, Hofmann, E., Gobets, B., van Stokkum, I. H. M., van Grondelle, R., Diederichs, K., van Amerongen, H.: **Forster excitation energy transfer in peridinin-chlorophyll-a-protein.** *Biophysical Journal* 2000, **78**(1):344-353.
23. van der Horst MA, Hellingwerf KJ: **Photoreceptor proteins, "star actors of modern times": a review of the functional dynamics in the structure of representative members of six different photoreceptor families.** *Acc Chem Res* 2004, **37**(1):13-20.
24. Anderson S, Dragnea V, Masuda S, Ybe J, Moffat K, E.Bauer C: **Structure of a novel photoreceptor, the BLUF domain of AppA from Rhodobacter sphaeroides.** *Biochemistry* 2005, **44**(22):7998-8005.
25. Bonetti C, Mathes T, van Stokkum IH, Mullen KM, Groot ML, van Grondelle R, Hegemann P, Kennis JT: **Hydrogen bond switching among flavin and amino acid side chains in the BLUF photoreceptor observed by ultrafast infrared spectroscopy.** *Biophysical Journal* 2008, **95**(10), 4790-4802.
26. Gauden M, van Stokkum IHM, Key JM, L ü hrs DC, van Grondelle R, Hegemann P, Kennis JTM: **Hydrogen-bond switching through a radical pair mechanism in a flavin-binding photoreceptor.** *P Natl Acad Sci USA* 2006, **103**(29):10895-10900.
27. Gomelsky M, Klug G: **BLUF: a novel FAD-binding domain involved in sensory transduction in microorganisms.** *Trends Biochem Sci* 2002, **27**(10):497-500.
28. Masuda S, Bauer CE: **AppA is a blue light photoreceptor that antirepresses photosynthesis gene expression in Rhodobacter sphaeroides.** *Cell* 2002, **110**(5):613-623.
29. Masuda S, Hasegawa K, Ishii A, Ono TA: **Light-induced structural changes in a putative blue-light receptor with a novel FAD binding fold sensor of blue-light using FAD (BLUF); Slr1694 of Synechocystis sp PCC6803.** *Biochemistry* 2004, **43**(18):5304-5313.
30. Masuda S, Hasegawa K, Ono TA: **Light-induced structural changes of apoprotein and chromophore in the sensor of blue light using FAD**

(BLUF) domain of AppA for a signaling state. *Biochemistry* 2005, **44**(4):1215-1224.

31. Unno M, Sano R, Masuda S, Ono TA, Yamauchi S: **Light-induced structural changes in the active site of the BLUF domain in AppA by Raman spectroscopy**. *Journal of Physical Chemistry B* 2005, **109**(25):12620-12626.
32. El Bissati K, Delphin E, Murata N, Etienne A, Kirilovsky D: **Photosystem II fluorescence quenching in the cyanobacterium Synechocystis PCC 6803: involvement of two different mechanisms**. *Biochim Biophys Acta* 2000, **1457**(3):229-242.
33. Holt TK, Krogmann DW: **A carotenoid protein from cyanobacteria**. *Biochim Biophys Acta* 1981, **637**:408-414.
34. Kerfeld CA: **Structure and function of the water-soluble carotenoid-binding proteins of cyanobacteria**. *Photosynth Res* 2004, **81**(3):215-225.
35. Kerfeld CA: **Water-soluble carotenoid proteins of cyanobacteria**. *Arch Biochem Biophys* 2004, **430**(1):2-9.
36. Wu YP, Krogmann DW: **The orange carotenoid protein of Synechocystis PCC 6803**. *Biochim Biophys Acta* 1997, **1322**(1):1-7.
37. Kerfeld CA, Sawaya MR, Brahmandam V, Cascio D, Ho, K. K., , Trevithick-Sutton CC, Krogmann DW, Yeates TO: **The crystal structure of a cyanobacterial water-soluble carotenoid binding protein**. *Structure* 2003, **11**(1):55-65.
38. van Stokkum IHM, Larsen DS, van Grondelle R: **Global and target analysis of time-resolved spectra**. *Biochim Biophys Acta* 2004, **1657**(2-3):82-104.